Spectroscopy of the solar Transition Region and Corona

L. Teriaca

The Solar Corona

Composite photo of the August 11, 1999 total eclipse. Lake Hazar, Turkey.

The Solar Corona

T_e=1 – 2 MK

Raw spectra obtained on 19 June 1936 during a total eclipse observed from the former Soviet Union.

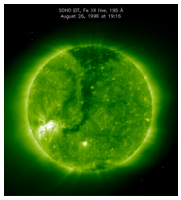

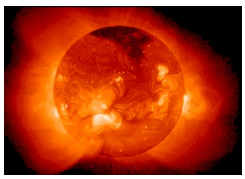

The Solar Chromosphere

T_e=10^4 K

Photo of the August 11, 1999 total eclipse. Kastamonu, Turkey.

The Solar Transition Region

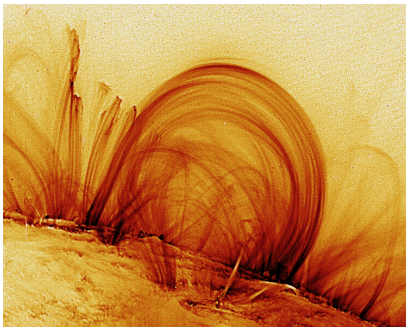

Radiant power density

Optically thin plasma

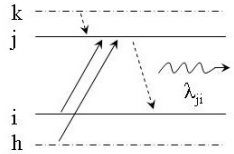

Spectral radiant power density: $P(\lambda)_{ji} = \frac{hc}{\lambda_{ji}} N_j A_{ji} \Psi(\lambda)$ $\left(\text{erg s}^{-1}\text{cm}^{-3}\text{Å}^{-1}\right)$

Radiant power density: $P_{ji} = \frac{hc}{\lambda_{ji}} N_j A_{ji}$ $\left(\text{erg s}^{-1}\text{cm}^{-3}\right)$

Radiant power density

$$P_{ji} = \frac{hc}{\lambda_{ji}} \frac{N_j}{N_{ion}} \frac{N_{ion}}{N_{el}} \frac{N_{el}}{N_H} \frac{N_H}{N_e} N_e A_{ji} \qquad \left(\text{erg s}^{-1}\text{cm}^{-3}\right)$$

$\frac{N_j}{N_{ion}}$ is the fraction of ions in the upper level j. **Strong function of N_e**

$\frac{N_{ion}}{N_{el}}$ is the relative abundance of the ionic specie. **Strong function of T_e**

$\frac{N_{el}}{N_H}$ is the element abundance with respect to hydrogen.

$\frac{N_H}{N_e}$ is the hydrogen to electrons number density ratio. ≈ 0.85

Radiant power density

Normalised radiant power density

$$\varepsilon_{ji} = \frac{P_{ji}}{N_{ion}} = \frac{hc}{\lambda_{ji}} \frac{N_j}{N_{ion}} A_{ji} \qquad \left(\text{erg s}^{-1}\right)$$

Contribution function

$$G\left(T_e, N_e, A_{el}\right)_{ji} = \frac{\varepsilon_{ji}}{N_e} \frac{N_{ion}}{N_{el}} \frac{N_{el}}{N_H} \frac{N_H}{N_e} \qquad \left(\text{erg s}^{-1}\text{cm}^{3}\right)$$

$$P_{ji} = G\left(T_e, N_e, A_{el}\right)_{ji} N_e^2 \qquad \left(\text{erg s}^{-1}\text{cm}^{-3}\right)$$

Line radiance

$$L_{ji} = \frac{1}{4\pi} \int_h G\left(T_e, N_e, A_{el}\right)_{ji} N_e^2 \mathrm{d}h \qquad \left(\text{erg s}^{-1}\text{cm}^{-2}\text{sr}^{-1}\right)$$

$$DEM(T) = N_e^2 \frac{\mathrm{d}h}{\mathrm{d}T} \qquad \left(\text{cm}^{-5}\text{K}^{-1}\right)$$

$$L_{ji} = \frac{1}{4\pi} \int_h G\left(T_e, N_e, A_{el}\right)_{ji} DEM(T) \mathrm{d}T \qquad \left(\text{erg s}^{-1}\text{cm}^{-2}\text{sr}^{-1}\right)$$

Differential emission measure

Atomic processes

Process	Rate ($\text{cm}^{-3}\ \text{s}^{-1}$)	Characteristic time (s)
Collisional excitation	$N_i N_e C_{ij}$	$2\ 10^{-3}$
Collisional deexcitation	$N_j N_e C_{ji}$	$2\ 10^{-3}$
Spontaneous radiative decay	$N_j A_{ji}$	$4\ 10^{-9}$
Collisional ionization	$N_e N_{ion} q_{coll}$	107
Radiative recombination	$N_e N_{ion} \alpha_{rad}$	88

Characteristic times for the relevant atomic processes in the Transition region as calculated for the C IV line at 154.8 nm (T_e=10^5 K, N_e=10^{10} cm^{-3}).

Thermal equilibrium

Te (K) \ Ne (cm^{-3})	5×10^8	10^{10}
10^5	τ_{ee}= 10^{-3} τ_{pp}= 0.04 τ_{ei}= 0.8	τ_{ee}= 5×10^{-5} τ_{pp}= 2×10^{-3} τ_{ei}= 0.04
10^6	τ_{ee}= 0.03 τ_{pp}= 1.3 τ_{ei}= 26	τ_{ee}= 0.02 τ_{pp}= 0.7 τ_{ei}= 1.3

Ionization (N_{ion}/N_{el})

$$\frac{dN^z}{dt} = N_e\left(N^{z-1}q^{z-1} + N^{z+1}\alpha_r^{z+1} + N^{z+1}\alpha_d^{z+1}\right) + -N_eN^z\left(q^z + \alpha_r^z + \alpha_d^z\right),$$

q	collisional ionization
α_r	radiative recombination
α_d	dielectronic recombination

ionization equilibrium → $\frac{dN^z}{dt} = 0$

$$\sum_{z=0}^{Z} N^z = N_{el}$$

Ionisation (N_{ion}/N_{el})

Excitation (N_j/N_{ion})

$$\frac{dN_i}{dt} = \sum_{j\neq i} N_jN_eC_{ji} - \sum_{j\neq i} N_iN_eC_{ij} + \sum_{j>i} N_jAji - \sum_{j<i} N_iAij,$$

statistical equilibrium → $\frac{dN_i}{dt} = 0$

$$\sum_i N_i = N_{ion}$$

Collisional rate coefficients

$$C_{ij} = \int_{v_0}^{\infty} \sigma_{ij}(v) f(v) v \, dv \qquad (\mathrm{cm}^3\ \mathrm{s}^{-1})$$

$$\sigma_{ij}(E) = \frac{\pi a_0^2 I_H \Omega_{ij}(E)}{\omega_i E},$$

$$\frac{dN(E)}{N_{Tot}} = \frac{2}{\sqrt{\pi}}(kT_e)^{-\frac{3}{2}}\sqrt{E}\exp\left(-\frac{E}{KT_e}\right)dE.$$

$$C_{ij} = \frac{8.63\times10^{-6}}{\omega_i kT_e^{\frac{3}{2}}}\int_{\Delta E_{ij}}^{\infty}\Omega_{ij}(E)\exp\left(-\frac{E}{kT_e}\right)dE,$$

$$C_{ij} = \frac{8.63\times10^{-6}\Omega_{ij}}{\omega_i T_e^{\frac{1}{2}}}\exp\left(-\frac{\Delta E_{ij}}{kT_e}\right).$$

Excitation (N_j/N_{ion})

Allowed transition: $\frac{N_j}{N_{ion}} \propto N_e \Rightarrow \frac{\varepsilon_{ij}}{N_e} = const$

Intersystem transition: $\frac{N_j}{N_{ion}} \propto N_e$ only if $N_eC_{ij} \ll A_{ji}$

$\frac{N_j}{N_{ion}} = const$ when $N_eC_{ij} \gg A_{ji}$

Excitation (N_j/N_{ion})

$$\varepsilon_{ji} = \frac{hc}{\lambda_{ji}}\frac{N_j}{N_{ion}}A_{ji}$$

CHIANTI atomic database: http:wwwsolar.nrl.navy.mil/chianti.html

Abundance (N_{el}/N_H)

$$A_{el} = \log \frac{N_{el}}{N_H} + 12$$

Table 4.2: Photospheric (Grevesse & Sauval 1998) and coronal (Feldman *et al.* 1992) element abundances for the most abundant element on the Sun. First Ionization Potentials (FIP) values are from Martin & Wiese (1996).

Element	Z	Photospheric	Coronal	FIP (eV)
H	1	12.00	12.00	13.59
He	2	10.93[a]	10.90	24.59
C	6	8.52	8.59	11.26
N	7	7.92	8.00	14.53
O	8	8.83	8.89	13.62
Ne	10	8.08[a]	8.08	21.56
Na	11	6.33	6.93	5.14
Mg	12	7.58	8.15	7.65
Al	13	6.47	7.04	5.99
Si	14	7.55	8.10	8.15
S	16	7.33	7.27	10.36
Ar	18	6.40[a]	6.58	15.76
Ca	20	6.36	6.93	6.11
Fe	26	7.50	8.10	7.90
Ni	28	6.25	6.84	7.64

[a] These abundances were determined using coronal data. However the Ne value is fully consistent with the result of Widing (1997), who measured it in photosphere.

Two – level atom

$$N_e N_g C_{gu} = N_u A_{ug}.$$

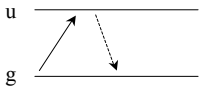

$$G(T_e)_{gu} = \frac{hc}{\lambda_{ug}} \frac{N_{ion}}{N_{el}} \frac{N_{el}}{N_H} \frac{N_H}{N_e} C_{gu}$$

$N_g = N_{ion}$

$$G(T_e)_{gu} = \frac{hc}{\lambda_{ug}} \frac{N_{ion}}{N_{el}} \frac{N_{el}}{N_H} \frac{N_H}{N_e} \frac{8.63 \times 10^{-6} \Omega_{ij}}{\omega_i T_e^{\frac{1}{2}}} \exp\left(-\frac{\Delta E_{ij}}{kT_e}\right).$$

Formation temperature

$T = 0.7 \times 10^4$ K

$T = 1.8 \times 10^5$ K

$T = 2.5 \times 10^5$ K

$T = 1.4 \times 10^6$ K

$T = 1.0 \times 10^6$ K

$T = 2.5 \times 10^5$ K

$T = 1.8 \times 10^5$ K

$T \approx 10^4$ K

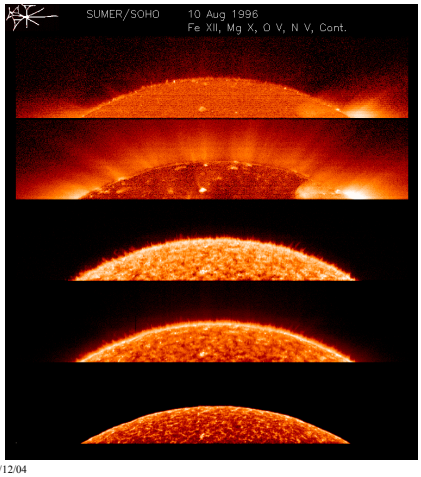

Emission Measure

$$L_{ji} = \frac{1}{4\pi} \int_h G(T_e)_{ji} N_e^2 dh \qquad (\text{erg s}^{-1}\text{cm}^{-2}\text{sr}^{-1})$$

$$\langle G(T_e)_{ji} \rangle = \frac{1}{T_{max}} \frac{\int_h G(T_e)_{ji} dh}{10^{(T_{max}+0.15)} - 10^{(T_{max}-0.15)}} \qquad (\text{erg s}^{-1}\text{cm}^3)$$

$$L_{ji} = \frac{\langle G(T_e)_{ji} \rangle}{4\pi} \int_h N_e^2 dh \qquad (\text{erg s}^{-1}\text{cm}^{-2}\text{sr}^{-1})$$

$$EM_c = \int_h N_e^2 dh \qquad (\text{cm}^{-5})$$

Electron density

$$EM_c = \int_h N_e^2 dh \qquad (cm^{-5})$$

$$\langle N_e^2 \rangle = \frac{4\pi L}{\langle G(T) \rangle} \frac{1}{fh}$$

Density sensitive line radiance ratio

$$R = \frac{\varepsilon_1}{\varepsilon_2} = f(N_e) \qquad \rightarrow \qquad f=10^{-2} - 10^{-5}$$

Coronal densities

Banerjee, Teriaca, Doyle, Wilhelm, 1998, A&A 339, 208

Electron temperatures

If we consider an isothermal plasma, the ratio of two allowed transitions from adjacent ionization stages reduces to the ratio of their contribution functions.

If we consider two allowed transitions from the ground state of the same ion:

$$\frac{I_{gk}}{I_{gj}} = \frac{\Delta E_{gk}}{\Delta E_{gj}} \frac{\Omega_{gk}}{\Omega_{gj}} exp\left(\frac{\Delta E_{gj} - \Delta E_{gk}}{kT_e}\right),$$

sensitive to the temperature if:

$$\left(\Delta E_{gk} - \Delta E_{gi}\right) \gg kT_e$$

Line profile

$$\Psi(\lambda) = \Psi(\lambda)_{NAT} * \Psi(\lambda)_{COLL} * \Psi(\lambda)_{Th} * \Psi(\lambda)_{Nth}$$

In the solar corona:

$$\Delta\lambda_{Th} = \Delta\lambda_{NAT} + \Delta\lambda_{COLL}$$

Assuming that the ions follow a Maxwellian distribution:

$$\Psi(\lambda)_{Th} = \frac{1}{\sqrt{\pi}\Delta\lambda_{Th}} \exp\left(-\frac{(\lambda - \lambda_0)^2}{\Delta\lambda_{Th}^2}\right)$$

where:

$$\Delta\lambda_{Th} = \frac{\lambda_0}{c} v = \frac{\lambda_0}{c}\left(\frac{2kT}{m_{ion}}\right)^{1/2}$$

Line profile

As an example, for N V 123.8 nm, (T_e=1.8×10^5 K),

$\Delta\lambda_{Th}$ = 0.061 Å = 14.9 km s^{-1}

However, we observe:

$\Delta\lambda_{Obs}$ = 0.143.8 Å = 34.8 km s^{-1}

$$\Delta\lambda_{Sun} = \frac{\lambda_0}{c}\left(\frac{2kT_e}{m_{ion}} + \xi^2\right)^{1/2} = \frac{\lambda_0}{c}\left(\frac{2kT_{eff}}{m_{ion}}\right)^{1/2}$$

Non–thermal velocity

Teriaca, Banerjee, Doyle, 1999, A&A, 349, 636

Doppler shift

Teriaca, Banerjee, Doyle, 1999, A&A, 349, 636

Chromospheric evaporation in flares

L. Teriaca et al.

Large upflows in CDS Fe XIX line at the footpoints of the flaring loop system during the impulsive phase.

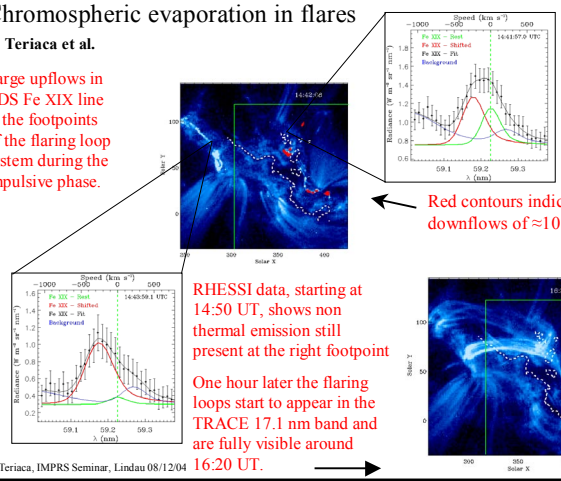

Red contours indicate Hα downflows of ≈10 km s^{-1}

RHESSI data, starting at 14:50 UT, shows non thermal emission still present at the right footpoint

One hour later the flaring loops start to appear in the TRACE 17.1 nm band and are fully visible around 16:20 UT.

Supersonic flows in a Quiet Sun loop

L. Teriaca et al. 2004, A&A 427, 1065

a) O VI SUMER raster of a small QS area. Black contours show magnetic flux of −10, −25, −40 G. Black + indicate the locations of strong non–Gaussian line profiles. The dashed red line indicates the projection on the plane of the sky of a semicircular loop with a diameter of 13". The black dots show the position of the observed loop.
b, d) Profiles on the legs of the loop with the results of a 3 component Gaussian fitting.
c) Profile at loop top. The dotted line shows the average QS profile times 4.9.
Observed speeds are consistent with the LOS component of a supersonic siphon–like flow of ≈130 km s^{-1} along the loop.